Combining the Calculus of Variations and Wavelets for Image Enhancement [1]

Ronald R. Coifman

Departments of Computer Science and Mathematics, Yale University, New Haven, Connecticut 06520

and

Artur Sowa

Department of Mathematics, Yale University, New Haven, Connecticut 06520

Communicated by Stephane G. Mallat

Received October 2, 1998; revised May 7, 1999

We propose methods of both slow and rapid post-processing of signals for erasure of artifacts that arise in the process of thresholding and quantization. We use wavelets as tools to define constraints and variational functionals as measures of complexity of signals. The methods come from analyses of different possibilities of blending variational calculus and wavelet multiresolution in ways that appear to be natural.

Key Words: image processing; image enhancement; denoising; data compression; wavelet optimization; wavelet shrinkage; wavelet relaxation.

1. INTRODUCTION

Given an imperfectly described signal, it is often the case that a few of its parameters are given with good precision whereas other parameters are known only vaguely or are *a priori* essentially unknown. If one believes, however, that the unknown parameters are somehow correlated with the known ones, then it is reasonable to try to extrapolate the unknown parameters from the available ones. This involves exploitation of additional, external principles of our choice — the ones that are believed to express relations between the two groups of parameters.

A good example of such a problem is provided by wavelet and wavelet packet-based techniques for denoising and compression of one- and two-dimensional signals. In one form or another, all these procedures use the following two steps. First, the signal is represented in some wavelet packet basis. In the second step, the coefficients of the representation are purposefully *altered* either to suppress noise or to compress the data,

[1] This research was supported by DARPA/AFOSR F49620-97-1-0011.

1063-5203/00 $35.00

or both. This is usually done by *thresholding* or *quantization* of coefficients. Thresholding in its most basic form means setting those coefficients that are smaller in absolute value than a certain threshold to zero. Quantization in its most basic form means rounding the coefficients off to the nearest multiple of a chosen unit (the quanta).

Efficient as these methods can be, they will unavoidably introduce undesirable artifacts to the processed signals. The artifacts become more and more manifest as the thresholding or quantization procedures get coarser.

Many methods of enhancement of noisy images using partial differential equations have been recently developed and tested. Among them, the method of Perona and Malik [8], the method of Alvarez *et al.* [1], and the method of Osher and Rudin [7] are perhaps representative (cf. [6] for a review and further references). One common feature of all of these methods is that they use nonlinear heat flows with the noisy image as the initial condition. Since, generally speaking, one expects heat flow to be a regularizing, smoothing process, it is necessary to take special precautions to prevent smoothing of the edges in the images. In order to achieve this, the authors mentioned above design nonlinear terms that enter the driving force sides of their equations to detect edges and slow down or stop dispersion in their direct vicinity. Let us point out a few shortcomings of these methods.

– Heat flow is a slow process.

– Even if the methods converged very rapidly, so that it would suffice to perform just a few steps in their discretized form, the nonlinearity would cause each step to be computationally expensive.

– None of these methods is applicable to erasure of artifacts that arise in the process of quantization or thresholding of images with the use of singular wavelets. Indeed, these procedures introduce artifacts in the form of edges. Therefore, any method of cleaning must have a way of distinguishing between the edges that are features of the original image and those that have been introduced artificially.

One approach to restoration of signals that have been subject to damage by thresholding would be to devise a method for extrapolation of coefficients below the threshold from those that remain unchanged above it. We will present here two mathematical treatments of this problem. The first one may be seen as a generalization of the method introduced by Bobichon and Bijaoui in their paper [2]. We believe that the second method is entirely new. It is in principle based on detection of wavelets (which are looked upon as undercurrent signals themselves) by matching with the use of specially designed correlation measures.

2. ALGORITHMS BASED ON THE STEEPEST DESCENT METHOD

The algorithms presented in this section are in their most interesting versions nonlinear, and as such usually quite slow. Nevertheless they are still interesting from the point of view of many particular applications. Below we give formal definitions of the processes we will simulate for the purpose of image enhancement. We emphasize that in what follows we will often stretch our initial definitions, discussing processes that require more general functional spaces for their consistent formulation. Since our main interest is in the discrete version of these processes, the latter issue has little merit.

Suppose now we are given two separable Hilbert spaces, H_1 and H_2, and a linear transform $T\colon\ H_1 \to H_2$. We assume that T is an isometry, i.e.,

$$\langle Tu_1, Tu_2\rangle = \langle u_1, u_2\rangle \qquad \text{for all } u_1, u_2 \in H_1.$$

We also fix orthonormal bases of the two Hilbert spaces as

$$H_1 = \overline{\text{span}\{\psi_i : i \in I\}} \qquad \text{and} \qquad H_2 = \overline{\text{span}\{e_i : i \in I\}},$$

assuming $T\psi_i = e_i$ with some discrete index see I. We do not specify any more properties of T, H_1, H_2 until later. However, we will think of T as a wavelet or wavelet-packet type transform. In addition, we think of H_1 as the physical space of signals and H_2 as the phase space. Furthermore, let Φ: $H_1 \to R$ be a (energy) functional defined over H_1 with some regularity that will be requested later. Let $M = \overline{\text{span}\{e_i : i \in J\}}$ for $J \subset I$ be a closed subspace, with P_M: $H_2 \to M$ the orthogonal projection into M and $P_{M^\perp}$: $H_2 \to M^\perp$ the orthogonal projection into the orthogonal complement of M. We are interested in the following problem. Given a $u_0 \in H_1$ and a $Q > 0$, find a $u_\infty \in H_1$ such that

$$\Phi(u_\infty) = \min_{u \in H_1} \Phi(u),$$

under constraint

$$P_M^\perp T(u_\infty - u_0) = 0 \qquad \text{and} \qquad |\langle Tu_\infty, e_i\rangle| \le Q \qquad \text{for all } i \in J.$$

We emphasize that this variational problem depends on the choice of basis. If the functional Φ is sufficiently regular to possess (at least formally) the gradient $\text{grad}\,\Phi$, one might attempt to solve this problem by the steepest descent method, i.e., by solving

$$\frac{\partial w}{\partial t} = -\Xi_{(-Q,Q)}(w) P_M T \,\text{grad}\,\Phi(T^{-1}w), \tag{1}$$

for $w \in H_2$ with the initial condition $T^{-1}w(0) = u_0$. Here we adopt the convention that multiplication by $\Xi_{(-Q,Q)}(w)$ is understood as the orthogonal projection into the subspace $\overline{\text{span}\{e_i : |\langle w, e_i\rangle| < Q\}}$, while reserving $\chi_{(-Q,Q)}$ to denote the characteristic function of the open interval $(-Q, Q)$. Equivalently, the flow (1) admits a dual formulation,

$$\frac{\partial u}{\partial t} = -T^{-1}\Xi_{(-Q,Q)}(Tu) P_M T \,\text{grad}\,\Phi(u), \tag{2}$$

with the initial condition $u(0) = u_0$. This abstract formulation of the flow (1) allows us to prove that the energy Φ decreases as the flow progresses.

PROPOSITION 1. *Suppose $u(t)$ is a solution of* (2) (*equivalently $Tu(t)$ is a solution of* (1)). *Then $t \to \Phi(u(t))$ is a decreasing function of time.*

Proof. Since T is an isometry, and both P_M and $\Xi_{(-Q,Q)}(Tu(t))$ are orthogonal projections, we obtain

$$\begin{aligned}\frac{d\Phi(u(t))}{dt} &= \left\langle \text{grad}\,\Phi(u), \frac{du}{dt}\right\rangle \\ &= -\langle \text{grad}\,\Phi(u), T^{-1}\Xi_{(-Q,Q)}(Tu) P_M T \,\text{grad}\,\Phi(u)\rangle \\ &= -\langle T\,\text{grad}\,\Phi(u), \Xi_{(-Q,Q)}(Tu) P_M T \,\text{grad}\,\Phi(u)\rangle \\ &= -||\Xi_{(-Q,Q)}(Tu) P_M T \,\text{grad}\,\Phi(u)||^2. \end{aligned} \tag{3}$$

This completes the proof. ■

The most important difference between the two equivalent dual formulations consists in the fact that whereas the evolution in the physical space (2) is given by a partial differential equation (and some extra integral operators), the evolution in the phase space (1) is given by an ordinary differential equation in the Hilbert space. This observation is fundamental for understanding convergence and the rate of convergence of these processes for different functionals Φ. Here, we will resolve this issue in detail in the case when Φ is a quadratic form, so that $\operatorname{grad}\Phi$ is a linear operator. We now assume that M is a finite dimensional linear subspace given by

$$M = \operatorname{span}\{e_i : i = 0, 1, \ldots, N-1\}.$$

Since only the M-component of w changes with time, we can assume that $w(t) = \sum_{i=0}^{N-1} a_i(t)e_i + w_r$, and equivalently $u(t) = \sum_{i=0}^{N-1} a_i(t)\psi_i + u_r$, where the remainders satisfy $w_r \in M^{\perp}$, $u_r = T^{-1}w_r \in T^{-1}(M^{\perp}) = T^{-1}(M)^{\perp}$. We now introduce the following notation.

$$A(t) = [a_0(t), a_1(t), \ldots, a_{N-1}(t)]^T$$

is the column of the evolving coefficients of w. Next we define an $N \times N$ matrix L by

$$L_{ij} = -\chi_{(-Q,Q)}(a_i)\langle \operatorname{grad}\Phi(\psi_j), \psi_i\rangle \qquad \text{for } i, j = 0, 1, \ldots, N-1.$$

Finally, we introduce the column vector

$$R(t) = -\begin{bmatrix} \chi_{(-Q,Q)}(a_0(t))\langle \operatorname{grad}\Phi(u_r), \psi_0\rangle \\ \chi_{(-Q,Q)}(a_1(t))\langle \operatorname{grad}\Phi(u_r), \psi_1\rangle \\ \vdots \\ \chi_{(-Q,Q)}(a_{N-1}(t))\langle \operatorname{grad}\Phi(u_r), \psi_{N-1}\rangle \end{bmatrix}.$$

A direct calculation shows that evolution equations (1) and (2) are equivalent to the system of ordinary differential equations

$$\dot{A}(t) = LA(t) + R(t). \tag{4}$$

Had it not been for the switching terms $\chi_{(-Q,Q)}(a_i(t))$ this system of ODEs would have been linear. Fortunately, the role of the switching terms can be easily described and we derive main properties of our flow from the well-understood theory of linear systems of ODEs. In fact we obtain the following theorem.

THEOREM 1. *Assume that Φ is a quadratic form in H_1, so that* $\operatorname{grad}\Phi$ *is a linear operator. Assume in addition that the linear subspace M is finite dimensional. Then the evolution given by* (1) *or* (2) *is completely determined by the bilinear form*

$$B(u, v) = -\langle u, \operatorname{grad}\Phi(v)\rangle \qquad \textit{for } u, v \in M.$$

In particular, if B is symmetric and negative definite, then the flow converges to a stable equilibrium, and the rate of convergence is at least $\exp(\lambda t)$, *where* $\lambda < 0$ *is the greatest eigenvalue of B. In addition, the flow is asymptotically stable.*

Proof. As we have pointed out above, the flows (1) or (2) are equivalent to the flow (4) with the initial condition $A(0)$. Consider the cube

$$C = \{[a_0, \ldots, a_{N-1}]^T : |a_i| < Q \text{ for } i = 0, 1, \ldots, N-1\}.$$

Redefining the linear space M if necessary, we can assume without loss of generality that $A(0) \in C$. Let us further denote

$$B_{ij} = -\langle \operatorname{grad} \Phi(\psi_j), \psi_i \rangle \qquad \text{for } i, j = 0, 1, \ldots, N-1,$$
$$R = -[\langle \operatorname{grad} \Phi(u_r), \psi_0 \rangle, \ldots, \langle \operatorname{grad} \Phi(u_r), \psi_{N-1} \rangle]^T.$$

For small time t the evolution is described by the linear system of ODEs $\dot{A}(t) = BA(t) + R(t)$. The vector $A(t)$ stays on the trajectory given by this system until at $t = t_1$ it first hits the boundary of the cube C. At that moment one or more of the factors $\chi_{(-Q,Q)}(a_i(t_1))$ switch to 0; e.g., $\chi_{(-Q,Q)}(a_i(t_1)) = 0$ for $i = i_1, i_2, \ldots, i_k$. After the moment t_1 the same process is repeated with a smaller subspace $M_1 = M \setminus \operatorname{span}\{e_i : i = i_1, i_2, \ldots, i_k\}$. Thus, the evolution (4) is given piecewise by linear systems of ODEs. In particular, if the bilinear form B is symmetric and negative definite, then the flow converges to a stable equilibrium point and it is asymptotically stable. This completes the proof. ■

Remark. Let us note that the effects of intertwining an elliptic differential operator with integral transforms as in $T \operatorname{grad} \Phi T^{-1}$ are far from trivial, let alone the nonlinear multiplication by an expression of the type $\Xi_{(-Q,Q)}(w)$. Indeed, it is a very instructive exercise to examine the one-dimensional case with the discrete linear second derivative $(u'')_i = u_{i+1} - 2u_i + u_{i-1}$ and T given by the Haar wavelet transform at one level. In fact, it is easily seen that for $w = w_H + w_G$, where w_H (w_G) are the low-pass (respectively high-pass) components of w, we have

$$T((T^{-1}w)'') = \begin{pmatrix} \phi_{HH} & \phi_{HG} \\ \phi_{GH} & \phi_{GG} \end{pmatrix} * \begin{pmatrix} w_H \\ w_G \end{pmatrix},$$

where $*$ denotes the convolution, and

$$\begin{aligned} \phi_{HH} &= (-1, 2, -1), \\ \phi_{HG} &= (1, 0, -1), \\ \phi_{GH} &= (-1, 0, 1), \\ \phi_{GG} &= (-1, -6, -1). \end{aligned}$$

This means that although the effect of $T((T^{-1}w)'')$ will be just an application of the second derivative to the low-pass component, it acts on the high-pass component by convolution with a smoothing kernel. In addition, there is some interaction between the channels. Similar behavior is observed with other wavelets as well. Of course, we should be aware of the fact that when $\operatorname{grad} \Phi$ is a nonlinear operator, the interaction between channels is difficult to control. On the other hand the flow given by Eq. (1) can be identified as the

projection of an ordinary heat flow to a subspace in H_1 that is subject to time evolution itself. Indeed, introducing $R_u = T^{-1} \circ \Xi_{(-Q,Q)}(Tu) P_M \circ T$, we obtain

$$\frac{\partial u}{\partial t} = -R_u \operatorname{grad} \Phi(u),$$

and we note that $R_u \circ R_u = R_u$ and, for orthogonal wavelets, $R_u^\star = R_u$. Moreover, as shown above, in the case of linear grad Φ there is a discrete sequence of times t_n at which the subspace $R_{u(t_n-\delta)}(H_1) \subset H_1$ switches to a smaller $R_{u(t_n+\delta)}(H_1) \subset H_1$ and the subspaces remain fixed in between.

THE ALGORITHM. The formula (1) is the one we actually convert into an algorithm in the case of thresholding. In the case of quantization it has to be modified to

$$\frac{\partial w}{\partial t} = -\Xi_{(-Q,Q)}(w - Tu_0) T \operatorname{grad} \Phi(T^{-1} w), \tag{5}$$

where the omission of P_M is deliberate. The algorithms are as follows.

1. Choose an energy functional, say Φ.
2. Pick T to be a wavelet or wavelet-packet transform according to what basis has been used to threshold or quantize the image.
3. If repairing a thresholded image set $M = \operatorname{span}\{\psi_i : \langle u_0, \psi_i \rangle = 0\}$, and let P_M denote the orthogonal projection into M.
4. Choose Q to be equal either to half the quanta or to the threshold.
5. Perform S steps of a discrete version of the evolution equation (1) in the case of thresholding and (5) in the case of quantization. S is to be chosen by experiment.

Remarks.

– In essence, a method roughly of this type (with $\Phi(u) = \int |\nabla u|^2$) was investigated in [2]. There, the algorithm is additionally required to proceed scale by scale and grad Φ is being evaluated not only in the physical space but also in the phase space.

– In some cases improvement in quality of the enhanced image can be obtained by replacing the wavelet transform by the undecimated (redundant) wavelet transform. Furthermore, the method extends to other redundant descriptions as well. For instance, interesting effects have been obtained by simultaneous use of several bases. In this case Eq. (1) has to be replaced by a system of two (several) equations of the form

$$\begin{aligned} \frac{\partial w_1}{\partial t} &= -\Xi_{(-Q_1,Q_1)}(w_1) P_{M_1} T_1 \operatorname{grad} \Phi(T_2^{-1} w_2) \\ \frac{\partial w_2}{\partial t} &= -\Xi_{(-Q_2,Q_2)}(w_2) P_{M_2} T_2 \operatorname{grad} \Phi(T_1^{-1} w_1), \end{aligned} \tag{6}$$

with $w_i \in H_2^i$, $T_i \colon H_1 \to H_2^i$, and $P_{M_i} \colon H_2^i \to M_i$ for $i = 1, 2$ are as above, and the initial conditions $T_i^{-1} w_i(0) = u_0 \in T_1^{-1} M \cap T_2^{-1} M$ are consistent.

– The algorithms presented above have one clear disadvantage. Since the gradient of the functional Φ does not have anything in common with the signal, the method of the steepest descent introduces its own artifacts. One-dimensional signals are usually smoothed, but on the other hand application of the algorithm can amplify the Gibbs phenomenon. For images we will observe edge and corner smearing, but also a

propagation-of-textures effect. All this depends heavily on the choice of a particular functional Φ. In the Appendix we present an example of the image thresholded in the Haar basis, which is then restored using $\Phi(u) = \int |\nabla u|^2$, and another one for $\Phi(u) = \int |\nabla u|$, in which case the operator grad Φ is approximated by

$$\operatorname{grad} \Phi(u) \sim \operatorname{div}\left(\frac{\nabla u}{(|\nabla u|^2 + \varepsilon^2)^{1/2}} \right),$$

for a small ε. To ensure regular behavior one needs to choose the time step unit less than $\varepsilon/10$. Of course, the results depend on the stopping time, although, experiment shows fast convergence.

3. ALGORITHMS BASED ON WAVELET-SHAPE DETECTION

In principle the algorithms presented in this section perform in computational time proportional to the size of the data set. However, the proportionality constant is so large that they are in practice much slower than the algorithms of the previous section. Nevertheless, we will show in the next section how to refine one type of these algorithms to a rapid and effective image-enhancement procedure. We recommend that this section be viewed as either a source of effective algorithms for one-dimensional signals or an introduction to the principles that are behind the construction of the rapid algorithm in the next section.

The present method attempts to take advantage of the fact that artifacts introduced by thresholding often resemble the wavelets themselves. More strictly, given initial signal u_0, both thresholding and quantization will add a bunch of wavelets to it, and the resulting signal has the form $u_1 = u_0 + \sum a_i \psi_i$. Our task then is defined as detection of the ψ_i's. Moreover, we know that a_i must satisfy constraints of the form $|a_i| < Q$, where either Q does not depend on i or we know how it depends on i. (The first possibility holds in the case of quantization and then $2Q$ is the quanta. The second possibility holds in the case of thresholding and then Q equals the threshold for those i for which $\langle u_1, \psi_i \rangle = 0$, and $Q = 0$ otherwise.)

THE ALGORITHM. We use many distinct ways of detecting correlation of shapes, but in all the cases, we proceed as follows.

1. Choose a measure of correlation, say C. $C(f, g)$ is a (bilinear or not) functional, which is assumed to measure how similar are (the shapes of) the two signals f and g.

2. Pick ε, consider $u_1 + \varepsilon\psi_i$ and $u_1 - \varepsilon\psi_i$. Consider all the ψ_i in the case of quantization and only those for which $\langle u_1, \psi_i \rangle = 0$ in the case of thresholding. Choose a threshold of correlation cor.

3. If $C(u_1, \psi_i) >$ cor update $u_1 = u_1 + \varepsilon\psi_i$, else if $C(u_1, -\psi_i) >$ cor update $u_1 = u_1 - \varepsilon\psi_i$, else do nothing at this ψ_i, consider the next ψ_i. Try all the wavelets ψ_i (or those which have been set to zero by thresholding) to reconstruct one ε layer.

4. Repeat the previous step Q/ε times; i.e., go through the total of Q/ε layers of reconstruction.

In the experiments whose results are presented below, we have used the following measures of correlation.

1. $C1$ is given by

$$C1(u_1, \psi_i) = -\frac{\int \langle u_1', \psi_i' \rangle}{(\int |u_1'|^2 \int |\psi_i'|^2)^{1/2}},$$

where $(.)'$ denotes the derivative.

2. $C2$ is given by

$$C2(u_1, \psi_i) = \int \kappa_{u_1} \kappa_{\psi_i},$$

where κ_f denotes the geodesic curvature of f, i.e.,

$$\kappa_f = \frac{f''}{(1 + f'^2)^{3/2}}.$$

Of course, depending on the specific application one can design functionals other than those presented above.

Remarks.

– The computational time required by the algorithm is $C(M/\varepsilon)N$. Here N is the number of ψ_i's we need to consider, which is equal to the signal length (or area for 2D) for quantization and smaller for thresholding. The constant C is basically the computational time required to perform step 3, which depends only on the chosen Φ.

– The signal one obtains in this way is quantized with the quanta equal to ε. A priori, the smaller ε, the better the results, but in practice exceeding exactness gives negligible improvement in quality of the signal.

– It has to be noted that the algorithm has built-in preference for $u_1 + \varepsilon\psi$ over $u_1 - \varepsilon\psi$ or vice versa, depending on which is being tested first. This affects the evolution of u_1 only at points where we are at a local maximum or a saddle point of the functional Φ. However, experiment shows that the effects of this bias are completely negligible for signals one encounters in practice.

– It is an attractive and convenient feature of this algorithm that it does not require any regularity of the functional Φ, since we do not need to know its gradient. The shortcoming of this algorithm is that if one attempts to use it actually to minimize the functional Φ, one has to successively refine the ε quantization. This poses nontrivial (even in finite dimensions) questions about convergence to the minimizer and, needless to say, the answer will depend on the properties of Φ. We emphasize, however, that it is not our task in this paper to minimize functionals, but to detect and erase artifacts of wavelet processing. For our purposes here, the issues just raised are irrelevant. What is more, the self-imposed limitations of this method are designed to play to our advantage.

– For our purposes, it always pays to choose the functional Φ that will in some sense emphasize the role of the building blocks ψ_i.

– In Fig. 1, we present the results obtained by application of this algorithm with two different energy functionals to one-dimensional signals. It has to be mentioned that in the case of, say, the functional $C1$, it is possible to use $C1(u_1, \psi_i)$ itself as a good candidate for the amplitude at ψ_i, and avoid the ε steps. We will explore this possibility in the next section. Let us now remark that, in fact, even if we deal with an expression that is not bilinear, as, for example, $C2$, it is still possible to produce a good candidate for the amplitude using the nonlinear projection, e.g., we can use the minimizer of

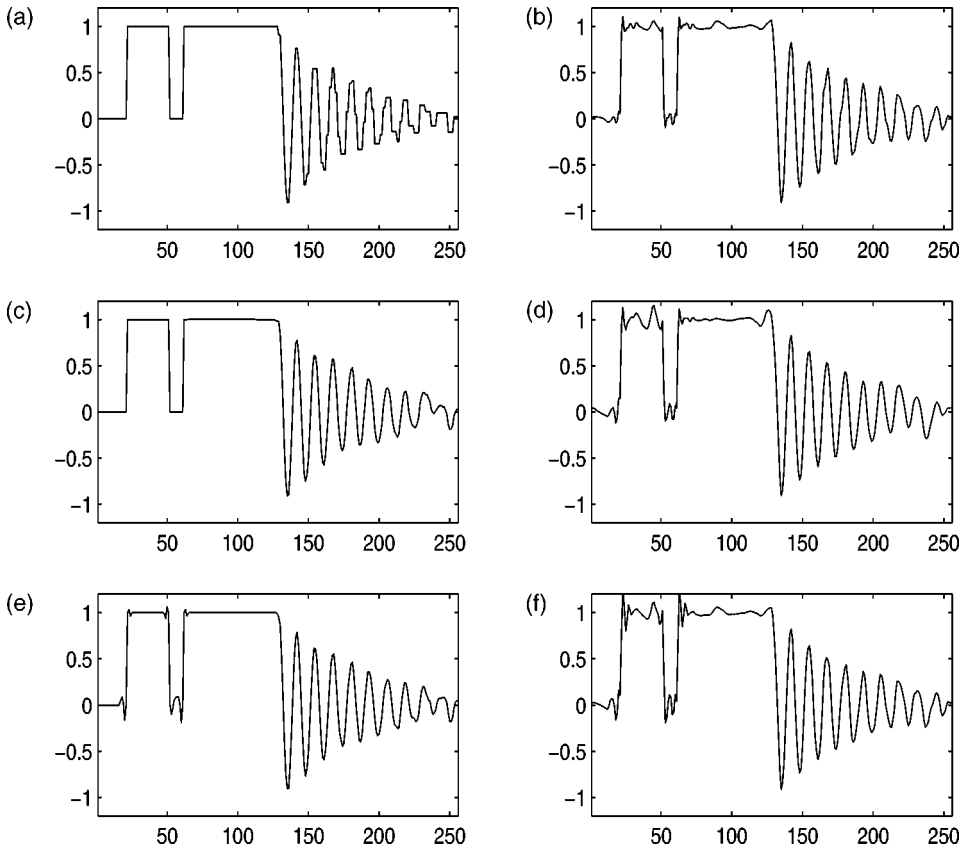

FIG. 1. (a) Signal thresholded in Haar basis, thresh $= 0.2$. (b) Signal thresholded in Daubechies8 basis, thresh $= 0.2$. (c) The signal from (a) restored using $C1$ and cor $= 0.01$. (d) The signal from (b) restored using $C1$ and cor $= 0.01$. (e) The signal from (a) restored using $C2$ and cor $= 0.02$. (f) The signal from (b) restored using $C2$ and cor $= 0.02$.

$\inf_\lambda \int |\kappa_{u_1+\lambda\psi_i}|^p$ for some $p \geq 1$. It is, however, more computationally expensive to minimize this nonlinear expression than to perform a large number of ε steps. Moreover, the experiment shows no improvement is achieved when this alteration is applied.

4. A RAPID ALGORITHM FOR ENHANCEMENT OF WAVELET COMPRESSED IMAGES

In this section we show how to devise a fast algorithm of the type presented above that proves to be especially effective for the Haar wavelet (making it a much more useful wavelet than expected). First, if we want to construct a rapid algorithm, we have to get rid of the ε and try to do all calculations simultaneously. This forces us to fix the amplitude of ψ_i at the optimal level once and for all. It seems natural to pick a_i such that

$$\Phi(u_0 + a_i\psi_i) = \inf_\lambda \Phi(u_0 + \lambda\psi_i).$$

This can be identified as performing one step toward the minimization of $\Phi(u)$ by the method of relaxation (cf. [4]). Second, in order to find the number a_i defined above numerically, we would usually have to spend a lot of time doing it, so it is desirable to obtain an explicit formula for a_i. Third, even if we succeed in obtaining such a formula, it still does not guarantee that its numerical evaluation will be fast enough. If we want it to be fast, the formula for a_i can only depend on a few coefficients of u_0 and ψ_i. All these conditions are met if we pick $\Phi(u) = \int |\nabla u|^2$. Indeed, then

$$\Phi(u_0 + \lambda\psi_i) = \int |\nabla u_0|^2 + 2\lambda \int \langle \nabla u_0, \nabla \psi_i \rangle + \lambda^2 \int |\nabla \psi_i|^2,$$

and the minimum is assumed for

$$\lambda = a_i = -\frac{\int \langle \nabla u_0, \nabla \psi_i \rangle}{\int |\nabla \psi_i|^2}.$$

The constants $\int |\nabla \psi_i|^2$ depend only on wavelets and can be precomputed. Moreover, the constants depend only on bands in the multiresolution table, which makes it possible to perform even this precomputation rather fast. More important, the numerators in the formula above are easy to compute if we integrate by parts to obtain

$$a_i = -\frac{\int \langle \Delta u_0, \psi_i \rangle}{\int \langle \Delta \psi_i, \psi_i \rangle}. \tag{7}$$

To justify integration by parts we make two remarks. First of all, we consider the pictures as functions on a two-dimensional torus, which is a closed manifold and therefore no boundary terms are present. We must add that we use a periodic wavelet transform in the applications, so that ψ_i's can be thought of as functions on the torus, too. Second, this integration by parts can be written down in the discrete version with the surface integral replaced by a double sum. This makes it retain its meaning in the digitized version. In summary, let u_0 be the image before processing, and let u_1 denote the image after processing. Let WT and IWT denote, respectively, the wavelet transform (inverse wavelet transform) in a fixed wavelet or wavelet packet basis.

THE ALGORITHM. The algorithm we propose consists of the following:

1. Find the wavelet coefficients $c_i = WT(u_0) = \langle u_0, \psi_i \rangle$.
2. Evaluate the finite difference Laplacian Δu_0.
3. Find the wavelet coefficients of the Laplacian

$$\tilde{\tilde{a}}_i = WT(\Delta u_0) = \langle \Delta u_0, \psi_i \rangle.$$

4. Rescale the coefficients $\tilde{\tilde{a}}_i$ according to the formula (7), dividing them by precomputed constants $\int |\nabla \psi_i|^2$. Obtain $\tilde{a}_i$.

5. Reset to zero those coefficients $\tilde{a}_i$ that do not satisfy the constraint. It means that if we are repairing a quantized image, we will put

$$a_i = \begin{cases} \tilde{a}_i & \text{if } |\tilde{a}_i| < Q \\ 0 & \text{otherwise.} \end{cases}$$

If, on the other hand, we are repairing a thresholded image, we will put

$$a_i = \begin{cases} \tilde{a}_i & \text{if } |\tilde{a}_i| < Q \text{ and } c_i = 0 \\ 0 & \text{otherwise.} \end{cases}$$

6. Define the restored image as

$$u_1 = IWT(c_i + a_i).$$

Remarks.

– The computational cost of the algorithm is essentially the cost of application of a filter corresponding to the Laplacian and twice the wavelet (or wavelet packet) and the inverse transform — once for the input signal u_0 and once for its Laplacian Δu_0. In addition every coefficient of the transform of the Laplacian Δu_0 has to be rescaled exactly once by a precomputed constant that depends only on the wavelets used and does not depend on the signal itself.

– In experiments we use with good results the simplest possible finite-difference Laplacian, i.e., if U is a matrix then with the common notation

$$(\Delta U)_{i,j} = U_{i+1,j} + U_{i,j+1} + U_{i-1,j} + U_{i-1,j-1} - 4U_{i,j}$$

with the obvious periodic extension at the boundary.

– Since the numbers we use for rescaling $\int |\nabla \psi_i|^2$ depend on the shape of ψ_i and not their position, they are constant within a given scale (or scale and band if wavelet-packets are used).

– If we were to look at this algorithm as a version of discrete heat flow restricted to certain scales and possibly bands, we would have to point out two distinctions. First, there is only one step in discrete time. The length of this step depends on the scale (band) and is given exactly by the number $(\int |\nabla \psi_i|^2)^{-1}$.

– Since multiplication of distributions is not well defined, the formula $\int |\nabla \psi_i|^2$ makes no sense for discontinuous Haar wavelets seen as functions of real variables. It can, however, be evaluated in the discrete version of wavelets, where ∇ denotes the left or right directional finite differences. The experiment shows that this works very well. In fact the existence of singularities may account for the fact that this method is most efficient for detection of artifacts left by the Haar wavelet.

Had we kept adding the wavelets one after another, we would have been sure that $\Phi(u_1) \leq \Phi(u_0)$. However, we have only used the functional Φ to compute the consecutive coefficients, and then we have added all the wavelets simultaneously. There is no *a priori* abstract reason for the value of the functional to go down. Below we prove that the L^2 variation will in fact decrease if one assumes in addition that the algorithm is restricted to a single band. More precisely, we consider a family of wavelets $\{\psi_i\}_{i=0}^{N-1}$ which are all shifts of a certain function. Thus in the one-dimensional case $\psi_i(x) = \psi(x - i)$ and in the two-dimensional case $\psi_i(x, y) = \psi(x - r, y - s)$, where $i = ns + r$, $n^2 = N$. In both cases we adopt the convention that the shift is circular, i.e.,

$$\psi_i(x) = \psi_{N-i}(x). \tag{8}$$

In particular, $\psi = \psi_0 = \psi_N$. We emphasize that N does not denote the size of the data set anymore. To avoid notational arithmetic we assume that there are N wavelets in the given band and the shifts are in fact dyadic multiplicities of the physical unit. All the statements below admit both continuous and discrete formulation. In the continuous case, it is sufficient that both ψ and its gradient $\nabla\psi$ be square integrable. Naturally, there is no regularity requirement in the discrete case. Let us introduce the matrix

$$M(i, j) = \frac{\int \langle \Delta\psi_i, \psi_j \rangle}{\int \langle \Delta\psi, \psi \rangle}. \tag{9}$$

In what follows, we will show that the property $\Phi(u_1) \le \Phi(u_0)$ follows from the following numerical property of wavelets.

NUMERICAL CONDITION 1.

$$\sum_{j=0}^{N-1} |M(0, j)| < 2.$$

The following fact is needed to prove Lemma 1. Even in one dimension, a formal proof of its validity would be purely descriptive and rather lengthy, let alone the two-dimensional version. Since in addition the fact has no mathematical subtlety of any kind and no other applications, we prefer to establish it by a numerical experiment.

EXPERIMENTAL FACT 1. *For all the discrete periodic compactly supported orthogonal wavelets, Numerical condition* 1 *is satisfied in both the one-dimensional and the two-dimensional cases.* (*In two dimensions we consider the so-called isotropic wavelet basis as opposed to the tensor product basis.*)

At this point we need to use the discrete Fourier transform and its basic properties. Here we just remind the definition. Given a vector $x = (x_0, x_1, \ldots, x_{N-1})$, by its discrete Fourier transform (DFT) we understand the vector $X = \mathrm{DFT}(x)$ given by

$$X_k = \sum_{l=0}^{N-1} x_l \exp\left(-\frac{2\pi\sqrt{-1}lk}{N}\right).$$

In what follows, we will need the following lemma.

LEMMA 1. *Numerical condition* 1 *implies that the quadratic form*

$$Q(x_1, x_2, \ldots, x_N) = -\sum_{i=1}^{N} x_i^2 + 2 \sum_{1 \le i < j \le N} x_i x_j M(i, j)$$

is negative definite, i.e.,

$$Q(x_1, x_2, \ldots, x_N) \le 0,$$

and the equality holds if and only if $x_1 = x_2 = \cdots = x_N = 0$.

Proof. Consider the matrix of the quadratic form

$$Q(i, j) = -2\delta_{i,j} + M(i, j),$$

where $\delta_{i,j}$ denotes the Kronecker delta. We note that since the Laplacian Δ is a symmetric operator, the matrix Q is also symmetric and in particular all its eigenvalues are real. Consider the one-dimensional case first. Since in this case ψ_i's are periodic shifts of each other, the matrix Q is circulant. It is well known that the eigenvalues of a circulant matrix are given by the discrete Fourier transform of one of its rows (cf. [5]), say $\lambda_k = \mathrm{DFT}(Q(0,j))$ for $k = 1, 2, \ldots, N$. In addition, $Q(0,j) = M(0,j) - 2\delta_{0,j}$ and $\mathrm{DFT}(\delta_{0,j}) = 1$. Thus, if Numerical condition 1 holds, then all the eigenvalues of Q are negative and the proof is completed. In the two-dimensional case M is not circulant any more. However, M consists of exactly n different $n \times n$ blocks that enter it in a circulant pattern and which themselves are circulant matrices. Thus, it follows from the general theory of circulant matrices (cf. [5, Theorem 5.8.1]) that M is diagonalizable, and its eigenvalues are linear combinations of the eigenvalues of the blocks, where the coefficients are all of modulus 1. More precisely, let λ_{ns+r} for $s, r = 0, 1, \ldots, n-1$ denote the eigenvalues of M, and let λ_k^l denote the kth eigenvalue of the lth block. (Since all the blocks are simultaneously diagonalizable by the DFT, there is a natural order in which the eigenvalues can be numbered.) In this notation

$$|\lambda_{ns+r}| = \left| \sum_{l=0}^{n-1} \exp\left(\frac{2\pi sl}{n-1}\right) \lambda_r^l \right| \le \sum_{l=0}^{n-1} |\lambda_r^l| \le \sum_{k=0}^{n^2-1} |M(0,k)| < 2,$$

where the last inequality follows from Numerical condition 1. Thus the form Q is negative definite and the proof is completed. ■

We are ready to prove the following.

THEOREM 2. *Assume about the algorithm above that only the wavelet coefficients at one band can be changed simultaneously. If Numerical condition* 1 *holds, then the energies of the output u_1 and the input u_0 in the case of both thresholding and quantization satisfy the inequality*

$$\int |\nabla u_1|^2 \le \int |\nabla u_0|^2,$$

with equality if and only if $u_1 = u_0$.

Proof. Suppose at first that all the coefficients $a_i = \int \langle \Delta u_0, \psi_i \rangle / \int |\nabla \psi|^2$ fall below the threshold (or within the quantization limit), i.e., the output u_1 is given by

$$u_1 = u_0 + \sum_{i=1}^{N} \frac{\int \langle \Delta u_0, \psi_i \rangle}{\int |\nabla \psi|^2} \psi_i = u_0 - \sum_{i=1}^{N} \frac{\int \langle \nabla u_0, \nabla \psi_i \rangle}{\int |\nabla \psi|^2} \psi_i.$$

We differentiate both sides of this equation and obtain as a result

$$\begin{aligned} \int |\nabla u_1|^2 &= \int \left| \nabla u_0 + \sum_{i=1}^{N} a_i \nabla \psi_i \right|^2 \\ &= \int |\nabla u_0|^2 - 2 \sum_i \frac{(\int \langle \nabla u_0, \nabla \psi_i \rangle)^2}{\int |\nabla \psi|^2} \\ &\quad + \sum_{i,j} \frac{\int \langle \nabla u_0, \nabla \psi_i \rangle \int \langle \nabla u_0, \nabla \psi_j \rangle \int \langle \nabla \psi_i, \nabla \psi_j \rangle}{(\int |\nabla \psi|^2)^2} \end{aligned}$$

$$= \int |\nabla u_0|^2 - \sum_i \frac{(\int \langle \nabla u_0, \nabla \psi_i \rangle)^2}{\int |\nabla \psi|^2}$$
$$+ 2 \sum_{i<j} \frac{\int \langle \nabla u_0, \nabla \psi_i \rangle \int \langle \nabla u_0, \nabla \psi_j \rangle \int \langle \nabla \psi_i, \nabla \psi_j \rangle}{(\int |\nabla \psi|^2)^2}$$
$$= \int |\nabla u_0|^2 + \frac{1}{\int |\nabla \psi|^2} \left(- \sum_{i=1}^{N} x_i^2 + 2 \sum_{1 \le i < j \le N} x_i x_j M(i,j) \right), \quad (10)$$

where $x_i = \int \langle \nabla u_0, \nabla \psi_i \rangle$. Thus, the claim follows from Lemma 1. We now examine what happens if some of the coefficients a_i are obtained by a nontrivial application of thresholding to the original correlation coefficients, i.e., let

$$\tilde{a_i} = \frac{\int \langle \nabla u_0, \nabla \psi_i \rangle}{\int |\nabla \psi|^2}$$

and let

$$a_i = \tilde{a_i} \chi_{\{|a_i| < Q\}}(\tilde{a_i}) \chi_{\{c_i = 0\}}(c_i),$$

in the case of thresholding, and let

$$a_i = \tilde{a_i} \chi_{\{|a_i| < Q\}}(\tilde{a_i}),$$

in the case of quantization, both for a given threshold Q (respectively quanta $2Q$). In both cases we denote $y_i = \int \langle \nabla u_0, \nabla \psi_i \rangle$, $x_i = \int |\nabla \psi|^2 a_i$, and note that $x_i y_i = x_i^2$. A similar calculation as above shows that now

$$\int |\nabla u_1|^2 - \int |\nabla u_0|^2 = \frac{1}{\int |\nabla \psi|^2} \left(-2 \sum_{i=1}^{N} x_i y_i + \sum_{i,j} x_i x_j M(i,j) \right)$$
$$= \frac{1}{\int |\nabla \psi|^2} \left(-2 \sum_{i=1}^{N} x_i^2 + \sum_{i,j} x_i x_j M(i,j) \right)$$
$$= \frac{1}{\int |\nabla \psi|^2} \left(- \sum_{i=1}^{N} x_i^2 + 2 \sum_{1 \le i < j \le N} x_i x_j M(i,j) \right) \le 0, \quad (11)$$

by Lemma 1, and the equality holds only if u_1 and u_0 are identical. This completes the proof. ■

Remarks.

– We emphasize that Theorem 2 depends nontrivially on properties of the wavelets used throughout. Indeed, consider the following problem. Suppose $u_1 = u_0 + c \Delta u_0$ for a certain constant $c > 0$. Can c be chosen independent of u_0 in such a way that always $\int |\nabla u_1|^2 \le \int |\nabla u_0|^2$? The answer is negative, which is easily seen if one plugs the eigenfunctions of the Laplacian corresponding to higher and higher eigenvalues in place of u_0. Next, it suffices to evaluate the integrals $\int |\nabla u_i|^2$ to see that the constant c will have to decrease to zero as the eigenvalues increase in order to guarantee the inequality, e.g., if $u_0 = \sin(2\pi k x)$, then $c < (2\pi k)^{-1}$.

– In practice we add the coefficients at all scales and bands simultaneously. Nevertheless, we have never observed gain of energy.

5. APPLICATIONS

We will indicate applications of the algorithm presented above to enhancement of images that have been thresholded or quantized, magnification of images, and last but not least, deblocking of images compressed with JPG software. In principle Fig. 5 is a good illustration of the kinds of effects that are obtained with all these mutations of the deblocking algorithm.

Dethresholding and dequantization. Experiment shows that the quality of restoration does not depend on whether the artifacts have been introduced by thresholding or quantization. The method does not depend on whether we use wavelet bases or wavelet packet bases, either. Similarly as in the case of one-dimensional signals, the improvement in quality of the image becomes less spectacular as the wavelets used for compression become more regular and blocking artifacts are replaced by ringing phenomena. This suggests an application of this method in processes that require high speed of computation, especially on the transmitter side, with reasonable image quality.

Magnification. For magnification of images, one takes the image as the low-pass of the Haar wavelets. After having performed the magnification by the inverse Haar transform, one applies the algorithm described above. No thresholding is necessary. The image has to be renormalized to amplify the energy.

DE-JPG. By DE-JPG we understand a mutation of our algorithm that allows us to *rapidly* deblock images compressed with JPG software. In fact in this version:

1. The algorithm performs three levels of the Haar transform (three because the JPG blocks have size 8-by-8).
2. The algorithm assumes the low-pass coefficients as accurate. (They are the average values of the image inside the 8-by-8 blocks.)
3. The algorithm extrapolates new high-pass coefficients using the principle explained in the previous section.
4. The algorithm automatically estimates the appropriate threshold level for a given image. (This is done using an empirical formula given in terms of the level of quantization of the low-pass coefficients of the JPG compressed image.)
5. The newly extrapolated coefficients are thresholded using the above estimate and are then added to the existing high-pass coefficients (but only where the latter ones are originally below the threshold).
6. The new image pixel values are reset between 0 and 255.

The automatic detection of the threshold can be optionally replaced by manual selection of the threshold. As a rule, the bigger the threshold the more smoothing should be expected. The automatic threshold is set so that it increases PSNR of the image in the known cases. The JPG-compressed images that have been post-processed with DE-JPG can be sharpened without emphasizing the 8-by-8 grid. This is in contrast to JPG compressed images, even for very low compression rates.

APPENDIX: EXAMPLES OF PROCESSED IMAGES

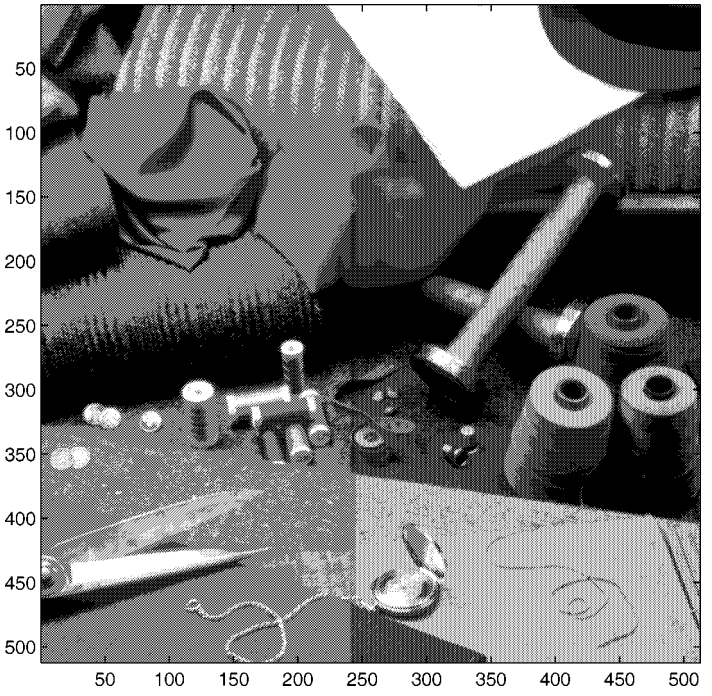

FIG. 2. Original image.

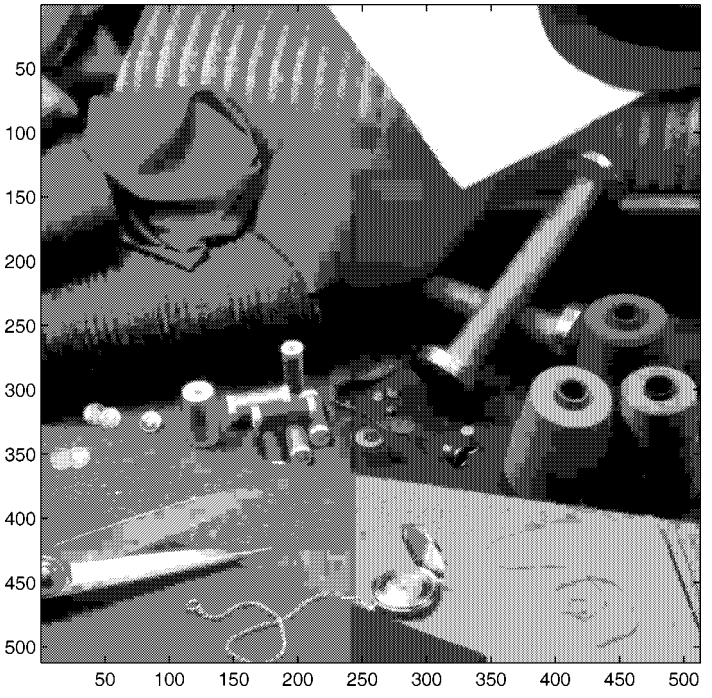

FIG. 3. Thresholded image, PSNR = 30.44.

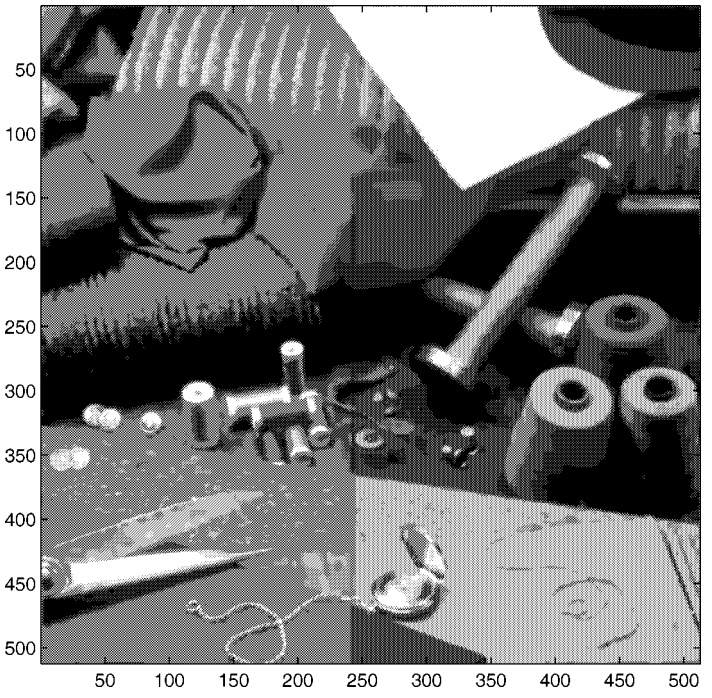

FIG. 4. Image restored using L2 variation, PSNR = 30.86.

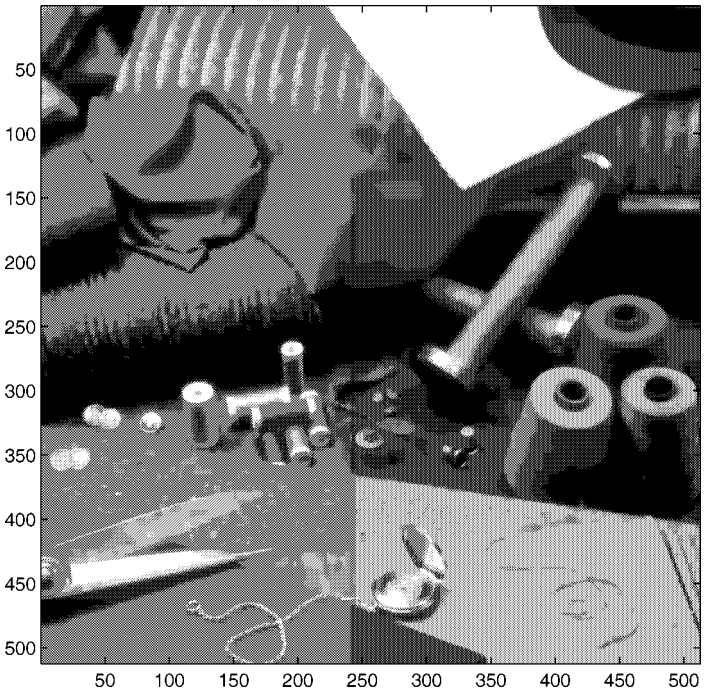

FIG. 5. Image restored using L1 variation, PSNR = 30.98.

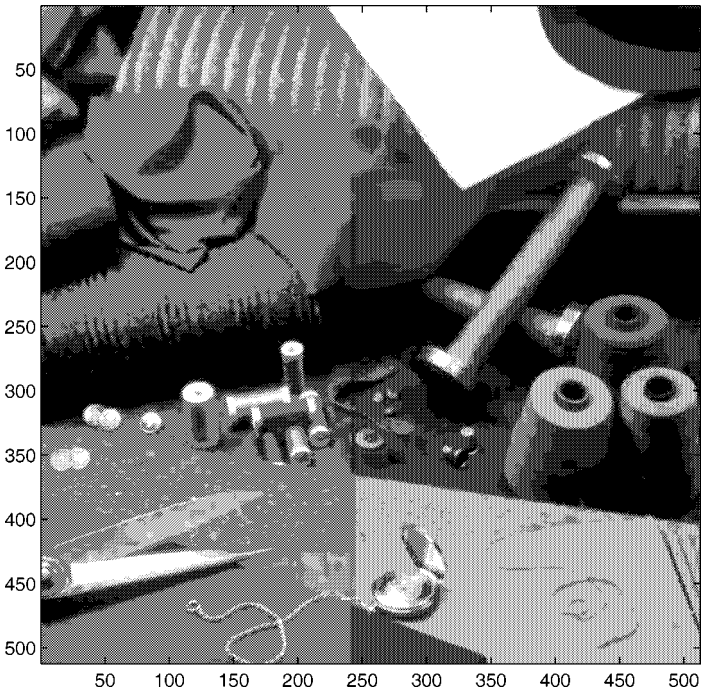

FIG. 6. Image restored using the rapid algorithm, PSNR = 31.48.

ACKNOWLEDGMENT

The authors thank Christopher Hatchell for help in editing the manuscript.

REFERENCES

1. L. Alvarez, P.-L. Lions, and J.-M. Morel, Image selective smoothing and edge detection by nonlinear diffusion, II, *SIAM J. Numer. Anal.* **29** (1992), 845–866.
2. Y. Bobichon and A. Bijaoui, Regularized multiresolution methods for astronomical image enhancement, *Exper. Astron.* **7** (1997), 239–255.
3. Y. Bobichon and A. Bijaoui, Regularization constraints in lossy compressed astronomical images restoration, *in* "Wavelet Applications in Signal and Image Processing IV, SPIE Conference," Denver, August 1996.
4. P. G. Ciarlet, "Introduction to Numerical Linear Algebra and Optimization," Cambridge University Press, Cambridge, UK, 1989.
5. P. J. Davis, "Circulant Matrices," Wiley, New York, Chichester, 1979.
6. J.-M. Morel and S. Solimini, "Variational Methods in Image Segmentation," Birkhäuser, Basel, 1995.
7. S. Osher and L. I. Rudin, Enhancement using shock filters, *SIAM J. Numer. Anal.* **27** (1990), 919–941.
8. P. Perona and J. Malik, Scale space and edge detection using anisotropic diffusion, *in* "Proc. IEEE Comput. Soc. Workshop on Comput. Vision," 1987.